Phys. Status Solidi C **7**, No. 9, 2306–2310 (2010) / **DOI** 10.1002/pssc.200983751

physica status solidi c
www.pss-c.com
current topics in solid state physics

$Zn_{1-x}Mg_xO$ thin films deposited by spray pyrolysis

M. Sahal, B. Marí*, M. Mollar, and F. J. Manjón

Institut de Disseny per la Fabricació Automatitzada (IDF)–Departament de Física Aplicada, Universitat Politècnica de València, Camí de Vera s/n, 46022 València, Spain

Received 16 June 2009, revised 27 January 2010, accepted 11 February 2010
Published online 14 June 2010

Keywords ZnMgO, spray pyrolysis, doping, structure, optical properties, band gap

* Corresponding author: e-mail bmari@fis.upv.es

This work reports on an analysis of the chemical composition, structural, and optical properties of Mg-doped zinc oxide (ZMO) thin films with Mg concentration up to 54 at. % and prepared by the spray pyrolysis technique from acetate precursors. Chemical analysis show that the [Mg]/[Zn] ratio incorporated into the films is higher than that present in the starting solution. X-ray diffraction, Raman scattering, and transmission measurements show that all samples exhibit a single phase wurtzite structure with a transmittance above 70% in the visible range. Increasing Mg content leads to an increase of the band gap energy from 3.23 in pure ZnO to 3.57 eV in films with 54 at % of Mg content.

1 Introduction Transparent conducting oxide (TCO) layers have been studied extensively due to their broad range of applications, including bulk acoustic wave devices, acoustic-optic devices, short-wavelength semiconductor diode laser, photovoltaic devices, and liquid crystal displays [1-5]. Among these TCOs, zinc oxide (ZnO) is a very promising candidate for future thin film technology due to their exceptional properties like its direct band gap (3.2 eV) with high transparency in the visible range [6], and its higher exciton binding energy (60 meV) compared to that of GaN [7].

Other interesting properties of ZnO are its structural stability to high-energy radiations, its good amenability to wet-chemical etching, and its easy of doping with a wide variety of ions for different applications. For instance, doping with group III elements (B, Al, Ga, and In) yields highly conductive thin films [8-10], while doping with Be, Mg, and Cd allows to shift the bandgap from deep UV to NIR.

Among the different dopants intended to extend the band gap of ZnO towards the deep UV region, Mg doping has a great potential because of the high luminescence efficiency observed in $Zn_{1-x}Mg_xO$ (ZMO) samples [11]. Mg doping has the advantage that Mg^{2+} has a similar ionic radius (0.57 Å) as that of Zn^{2+} (0.60 Å) [12], therefore Mg ions have a large solubility in ZnO so the wurtzite structure of ZMO layers has been extensively studied.

Many researchers have successfully reported the growth of ZMO thin films with wurtzite structure by several technique depositions such as pulsed-laser deposition (PLD) [13], laser molecular-beam epitaxial (L-MBE) [14], metal organic chemical vapor deposition (MOCVD) [15], radio frequency magnetron sputtering [16], spray pyrolysis [17] and dip coating [18]. The spray pyrolysis technique is an excellent method for the deposition of thin films of metallic oxides. This technique has some advantages in comparison to the other methods: it is cheap to handle; no sophisticated elements or instruments are required; it is well adapted for mass fabrication; and it is easy to include in an industrial production line to produce large area coatings without the need of ultra high vacuum.

In this paper we study the effect of Mg doping on the chemical composition and the structural and optical properties and of ZMO layers deposited onto pyrex substrate by spray pyrolysis. We will show that wurtzite-type ZMO thin films can be easily prepared by spray pyrolysis and that their optical properties can be tuned by adjusting the Mg content.

2 Experimental details $Zn_{1-x}Mg_xO$ thin films with different [Mg]/[Zn] ratio were deposited by spray pyrolysis onto pyrex substrates which were previously washed with HNO_3 and subsequently rinsed with water, ethanol and acetone. To prepare the spray mixture, zinc chloride [$ZnCl_2$] and magnesium chloride hexahydrate

[$MgCl_2$:$6H_2O$] were used as sources of zinc and magnesium, respectively. They were dissolved into a 4:1 mixture of bidistilled water and ethanol to which a few drops of HCl were added till the solution reaches $15 \cdot 10^{-2}$ M. In order to vary the Mg concentration in the ZMO films the magnesium acetate tetrahydrate concentration was varied between 9 at. % to 33 at. % in the starting solution. The deposition conditions were the following: (i) the substrate temperature was maintained at 300±3 ºC; (ii) the solution flow rate and gas pressure were kept constant at 4ml/min and 1.5 bar respectively; iii) finally, the nozzle-substrate distance was kept to 30 cm and the spraying time was 20 min.

The chemical, structural, and optical properties of the as-grown ZMO thin films have been characterized with different techniques. Chemical properties have been characterized by microanalysis using energy dispersive X-ray spectroscopy (EDS) with a JEOL-JSM6300 scanning electron microscope operating at 10 kV. Structural properties were characterized by means of X-ray diffraction (XRD) measurements with a Rigaku Ultima IV diffractometer in the θ-2θ configuration and using CuK_α radiation (1.5418 Å). Structural properties were also characterized by Raman scattering measurements performed with a LabRAM HR UV spectrometer coupled to a Peltier-cooled CCD camera and using a 532 nm laser excitation line with 3 cm^{-1} spectral resolution. Finally, optical characterization of the films was performed by means of transmittance measurements using a Deuterium-Halogen lamp (DT–MINI–2–GS Micropark) in association with an HR-4000 Ocean Optics USB spectrometer optimized for the UV–VIS range.

3 Results

3.1 Chemical properties

Figure 1 shows the EDS spectra of two ZMO films corresponding to starting solutions containing 23 and 33 at. % of Mg, respectively. A peak corresponding to Mg, that increase proportionally with the Mg content, can be clearly observed and confirm the presence of this element in the sprayed films. EDS measurements were performed on different sites of the films and no considerable changes in the EDS spectra were found; thus indicating a good homogeneity in chemical composition of the films.

EDS measurements have allowed to calculate the Mg molar fraction (X_f=[Mg]/([Mg]+[Zn]) present in the thin films. The Mg molar fraction in our films has been found to vary between 0 and 0.54. Figure 2 shows the variation of Mg molar fraction in the films as a function of Mg molar fraction in the starting solution. A linear relationship with a 1.88 slope was found which indicates that the molar fraction in the films is approximately 2 times larger than that in the starting solution. This result can be understood by the higher melting point of Mg (650 ºC) than that of Zn (419.5 ºC). The rather different melting point leads to a larger evaporation of Zn and results in a higher concentration of Mg with respect to Zn in the sprayed samples than in the starting solution. Similar results were found in films prepared by PLD [19].

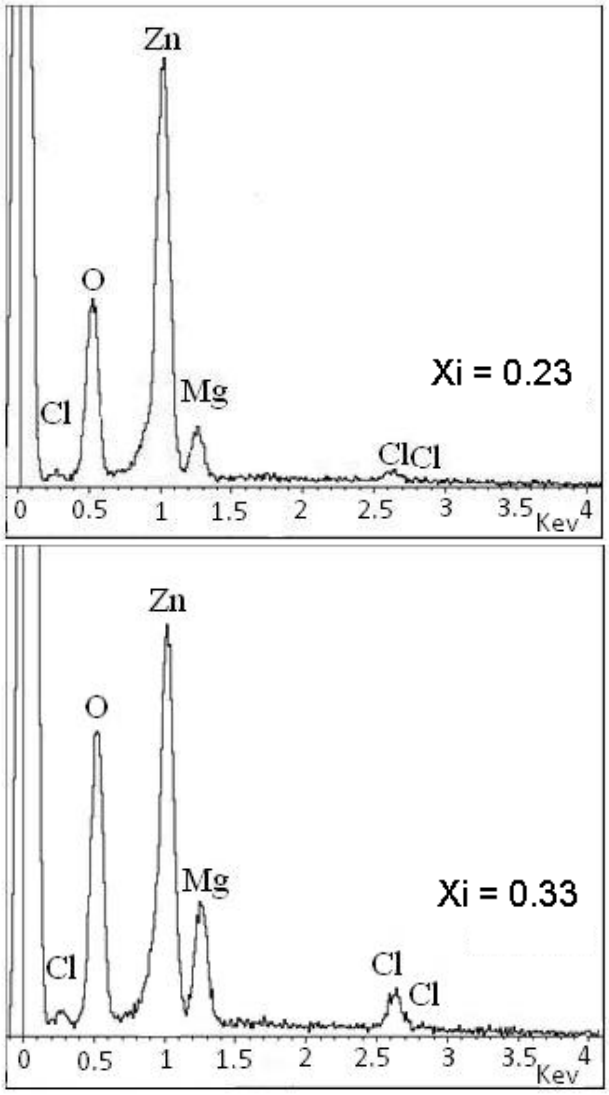

Figure 1 EDS spectra of ZMO sprayed films at 300 ºC with different Mg molar fraction in starting solution.

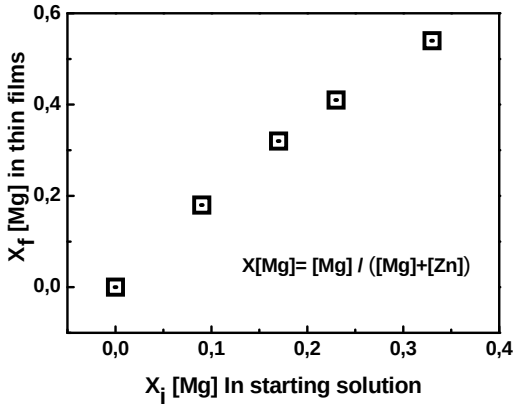

Figure 2 Mg molar fraction (X_f) in the ZMO thin films as a function of the Mg molar fraction in the starting solution (X_i).

3.2 Structural properties Figure 3 shows the XRD patterns of the ZMO thin films. All obtained films up to 54 at % of Mg were polycrystalline with a single phase of hexagonal symmetry (phase zincite JCPDS 36-1451) [20]. On the basis of the width of the peaks, they exhibit rather good crystal quality that decreases on increasing the Mg content and show a preferred orientation following the c-axis perpendicular to the substrate along the (002) direction. Our results are in agreement with those of ZMO films previously synthesized by MBE, PLD, and MOVPE techniques that also show the incorporation of a high Mg concentration between 33 and 49 at % [15, 21-23]. It is worth to note that we have measured a slight shift of the (002) diffraction peak towards higher angles from 34.32° (X_f=0) to 34.54° (X_f=0.54). Some authors attribute this shift to a substitution of zinc by magnesium in the hexagonal lattice [24]. In fact, an increase of the angle corresponding to the (002) reflection indicates a decrease of the c lattice parameter of the wurtzite structure.

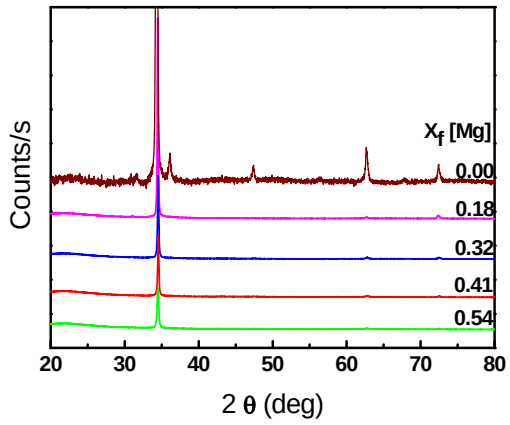

Figure 3 XRD spectra of ZMO thin films with different Mg molar fraction.

Figure 4 shows the variation of the c lattice parameter as a function of the Mg molar fraction as obtained from the (002) reflection of our XRD data with the expression

$$c=\lambda/\sin\theta \quad (1)$$

Figure 5 shows the Raman scattering measurements of ZMO thin films for different magnesium concentrations. The Raman spectrum of the ZMO films is similar to that of wurtzite-type ZnO. It exhibits two rather intense bands at 96.5 and 438 cm^{-1}, corresponding to the E_2(low) and E_2 (high) first-order Raman modes, and two rather broad bands centered around 330 and 574 cm^{-1} that correspond to the TO-TA (or E_2(high)-E_2(low)) second-order mode and the A_1(LO) first-order mode of ZnO, respectively [25]. With increasing Mg concentration up to 54 at. %, the E_2(low) mode increases slightly in width and shifts to smaller wavenumbers and the E_2(high) mode evidences a slight redshift and a considerable decrease in intensity. This behaviour of the E_2(high) mode and the increase in width of the broad band extending from 380 to 550 cm^{-1}, and corresponding to first-order scattering induced by defects [26] evidence a decrease of the crystal quality of the wurtzite structure of the films with increasing Mg content.

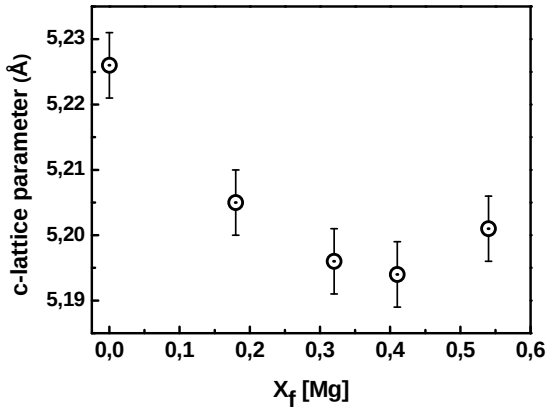

Figure 4 Dependence of the c lattice parameter as a function of the Mg molar fraction in the ZMO thin films.

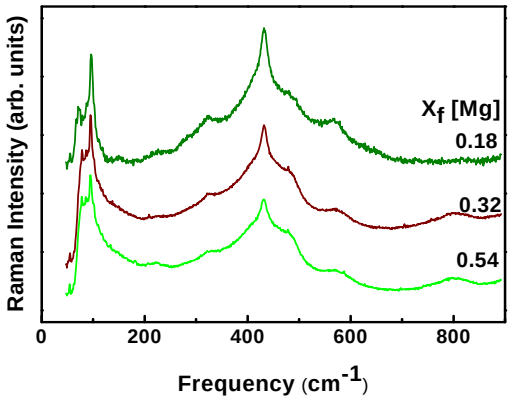

Figure 5 Raman scattering measurements of ZMO thin films with different Mg molar fraction.

A similar behaviour was previously observed in films doped with aluminium [26]. On the other hand, there is a considerable blueshift of the A_1(LO) mode (580 cm^{-1} for the sample with 54 at % Mg) that is in good agreement with previous reports on ZMO [27]. According to a recent interpretation of the Raman modes in wurtzite-type structures [28], the blueshift of the A_1(LO) mode can be explained by a decrease of the Zn-O bond distance along the c axis due to the decrease of the c lattice parameter with increasing Mg concentration. This result agrees with the decrease of the c-lattice parameter estimated from our XRD measurements and depicted in Fig. 4. Finally, the small redshift of both E_2 modes can be understood on the

light of a small increment of the Zn-O bond distance in the a-b plane of the wurtzite lattice [28]. A decrease of the c-lattice constant and increase of a lattice constant is in good agreement with previous results on ZMO [22].

3.3 Optical properties Figure 6 shows the optical transmittance spectra of our ZMO layers for different Mg concentrations as a function of wavelength in the range from 220 to 600 nm. The spectra show excellent transmission (above 70%) in the visible range of the optical spectrum and have a sharp absorption in the UV region. The absorption edge shifts towards the short wavelength region as the Mg content increases evidencing the substitutional incorporation of Mg into the Zn site of the wurtzite lattice.

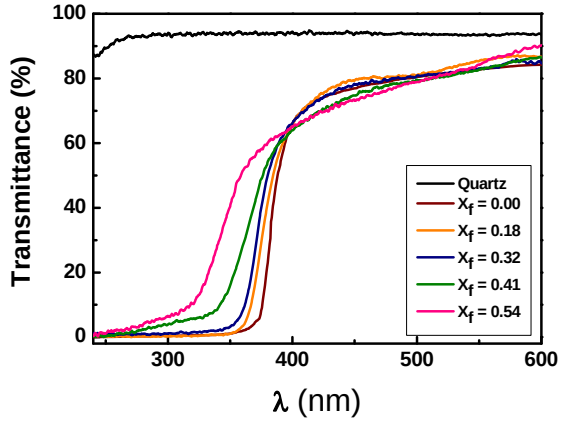

Figure 6 Optical transmittance spectra of $Zn_{1-x}Mg_xO$ thin films with different Mg molar fractions.

Since the ZnO is a semiconductor with a direct optical bandgap, the optical absorption coefficient, α, satisfies the expression [29, 30]

$$(\alpha h\nu)^2 = A(h\nu - E_g) \qquad (2)$$

where A is a constant, hν is the energy of the incident photon, and E_g is the bandgap energy that can be estimated by extrapolating the linear region of the $(\alpha h\nu)^2$ *vs* (hν) plot to α = 0.

Figure 7 shows the plot of $(\alpha h\nu)^2$ *vs* (hν) with the extrapolations used to estimate the bandgap in our ZMO films. A direct bandgap energy of 3.23 eV was found for undoped ZnO film in good agreement with the value of pure bulk ZnO [6]. The value of bandgap energy for the ZMO films shifted from 3.33 eV (X_f=0.18) to 3.57 eV (X_f=0.54) evidencing that the Mg^{2+} is successfully incorporated into the ZnO lattice in the Mg-doped ZnO films grown by spray pyrolysis. It is interesting to note that the blue-shift of the band gap energy measured on our ZMO films coincides with that reported by Kim and Seshadri and others [17, 31, 32]. However, it has been shown that the band gap of ZMO may change with Mg concentration from 3.2 eV in ZnO up to the upper limit of around 4.05 eV for Mg contents around 50 at. % [15, 32-38]. Therefore, the small bandgap blueshift observed in our ZMO films could likely indicate that not all the Mg cations in the films are substitutionally incorporated in the Zn cation sites. Assuming a linear rate for the change of the bandgap with Mg incorporation in the Zn sites and that sample with 50 at. % should exhibit a bandgap around 4.05 eV instead of 3.57 eV, we can estimate that only a 19 at. % of Mg out of 54 at. % is actually incorporated substituting Zn in our more doped films.

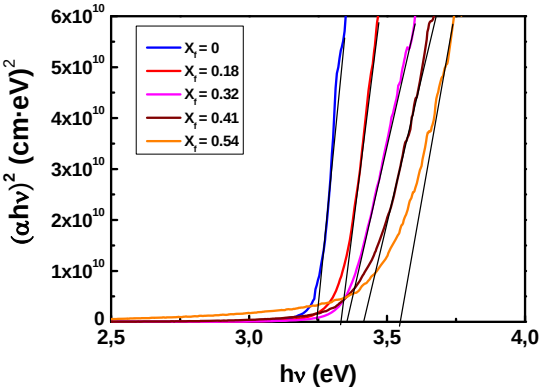

Figure 7 $(\alpha h\nu)^2$ vs. photon energy for $Zn_{1-x}Mg_xO$ sprayed thin films with different Mg molar fraction.

4 Conclusions This work shows the possibility to prepare wurtzite-like ZMO thin solid films over pyrex glass up to 54 at. % of Mg using the spray pyrolysis technique at 300 ºC. EDS measurements of the films have confirmed the incorporation of the Mg content with a higher molar fraction of this element in the layers than that in starting solution. X-ray diffraction and Raman scattering measurements reveal the wurtzite structure of the films and evidence a decrease in the film quality with increase of Mg doping. Finally, optical absorption measurements show an increase of the optical gap of the films as a result of the incorporation of Mg substituting Zn in the ZnO lattice. However, the smaller increase of the bangap than that observed in films prepared by other techniques suggests that not all the Mg incorporated in the as-grown films is substituting Zn in the ZnO lattice.

Acknowledgements This work was supported by Spanish Government through MICINN grant MAT2009-14625-C03-03.

References

[1] C. Guillén and J. Herrero, Thin Solid Films **480/481**, 129 (2005).
[2] M. Emziane, K. Durose, N. Romeo, A. Bosio, and D.P. Halliday, Thin Solid Films **480/481**, 377 (2005).
[3] M. Ohyama, H. Kozuka, T. Yoko, and S. Sakka, J. Ceram. Soc. Jpn. **104**, 296 (1996).

[4] D. Bao, H. Gu, and A. Kuang, Thin Solid Films **312**, 37 (1998).
[5] I. Z. K. Tang, G. K. L. Wong, P. Yu, M. Kawasaki, A. Ohtomo, H. Koinuma, and Y. Segawa, Appl. Phys. Lett. **72**, 3270 (1998).
[6] G.H. Lee, Y. Yamamoto, M. Kourogi, and M. Ohtsu, Thin Solid Films **386**, 117 (2000).
[7] K. Hümmer, Phys. Status Solidi B **56**, 249 (1973).
[8] J. H. Lee and B. O. Park, Thin Solid Films **426**, 94 (2003).
[9] H. Kim, A. Pique, J. S. Horwitz, H. Murata, Z. H. Kafafi, C. M. Gilmore, and D.B. Chresey, Thin Solid Films **377/378**, 798 (2000).
[10] J. H. Lee and B. O. Park, Mater. Sci. Eng. B **106,** 242 (2004).
[11] D.C. Look, Mater. Sci. Eng. B **80**, 383 (2001).
[12] R. D. Shannon, Acta Crystallogr. A **32**, 751 (1976).
[13] T. Makina and Y. Segawa, Appl. Phys. Lett. **78**, 1237 (2001).
[14] A. Ohtomo, K. Tamura, and K. Saikusa, Appl. Phys. Lett. **75**, 2635 (1996).
[15] W. I. Park, G.C. Yi, and H.M. Jang, Appl. Phys. Lett. **79**, 2022 (2001).
[16] Y. Miyazaki, M. Onoda, T. Oku, M. Kikuchi, Y. Ishii, Y. Ono, Y. Morii, and T. J. Kajitani, Phys. Soc. Jpn.**71**, 491 (2002).
[17] X. Zhang, X. M. Li, T. L. Chen, J. M. Bian, and C.Y. Zhang. Thin Solid Films **492**, 248 (2005).
[18] T. Minemoto, T. Negami, S. Nishiwaki, H. Takakura, and Y. Hamakawa,Thin Solid Films **372**, 173 (2000).
[19] C. Bundesmann, M. Schubert, A. Rahm, D. Spemann, H. Hochmuth, M. Lorentz, and M. Grundmann, Appl. Phys. Lett. **85**, 905 (2004).
[20] Powder Diffraction File Data Card 5-644, 3cPDS International Center for Diffraction Data, Swartmore, PA.
[21] A.K. Sharma, J. Narayan, J.F. Muth, C.W. Teng, C. Jin, A. Kvit, R.M. Kolbas, and O.W. Holland, Appl. Phys. Lett. **75**, 3327 (1999).
[22] A. Ohtomo, M. Kawasaki, T. Koida, K. Masubuchi, H. Koinuma, Y. Sakurai, Y. Yoshida, T. Yasuda, and Y. Segawa, Appl. Phys. Lett. **72**, 2466 (1998).
[23] A. Ohtomo, M. Kawasaki, Y. Sakurai, I. Ohkubo, R. Shiroki, Y. Yoshida, T. Yasuda, Y. Segawa, and H. Koinuma, Mater. Sci. Eng. B **56**, 263 (1998).
[24] S.C. Su, Y.M. Lu, Z.Z. Zhang, B.H. Li, D.Z. Shen, B. Yao , J.Y. Zhang, D.X. Zhao, and X.W. Fan, Appl. Surf. Sci. **254**, 4886 (2008).
[25] J. Serrano, A. H. Romero, F.J. Manjón, R. Lauck, M. Cardona, and A. Rubio, Phys. Rev. B **69**, 094306 (2004).
[26] A. El Manouni, F.J. Manjón, M. Mollar, B.Marí, R. Gómez, M.C. López, and J.R. Ramos-Barrado, Superlattices Microstruct. **39**, 185 (2006).
[27] C. Budesmann, A. Rahm, M. Lorenz, M. Grundmann, and M. Schubert, J. Appl. Phys. **99**, 113504 (2006).
[28] F.J. Manjón, D. Errandonea, A.H. Romero, N. Garro, J. Serrano, and M. Kuball, Phys. Rev. B **77**, 205204 (2008).
[29] W. Plaz, G. Cohen Solal, J. Vedel, J. Fermy, T. N. Duy, and J. Volerio, Proc. 7th IEEE Photov. Spec. Conf. Pasadena 54 (1968).
[30] E. Johnson, R. K. Willardardson, and A.C. Beer (Eds.) (Academic Press, New York, 1967), p. 157.
[31] Y. Kim and R. Seshadri, Inorg. Chem. **47**, 8437-8443 (2008).
[32] W. Yang, R.D. Vispute, S. Choopun, R.P. Sharma, T. Venkatesan, and H. Shen, Appl. Phys. Lett. **78**, 2787 (2001).
[33] S. Muthukumar, J. Zhong, Y. Chen, and Y. Lu, Appl. Phys. Lett. **82**, 742 (2003).
[34] Y.Z. Zhang, J.H. He, Z.Z. Ye, L. Zou, J.Y. Huang, L.P. Zhu, and B.H. Zhao, Thin Solid Films **458**, 161 (2003).
[35] Y. Matsumoto, M. Murakami, Z. Jin, A. Ohotomo, M. Lippmaa, M. Kawasaki, and H. Koinuma, Jpn. J. Appl. Phys. **38**, 603 (1999).
[36] T. Minetomo, T. Negami, S. Nishikawa, H. Takakura, and Y. Hamakawa, Thin Solid Films **372**, 173 (2000).
[37] Y. Chen, H. Ko, S. Hong, T. Sekiguchi, T. Yao, and Y. Segawa, J. Vac. Sci. Technol. B **18**, 1514 (2000).
[38] S. Choopun, R.D. Vispute, W. Yang, R.P. Sharma, T. Venkatesan, and H. Shen, Appl. Phys. Lett. **80**, 1529 (2002).

